Supplemental Material

Supplemental Material for: Robust responses of the Sahelian hydrological cycle to global warming

Spencer A. Hill, Yi Ming, and Ming Zhao

Correspondence: shill@atmos.ucla.edu

This document contains the following figures:

1. Figure S1: Sahel region-mean meridional MSE advection profiles and its components in the GFDL models, in the control simulations and in response to the imposed uniform SST warming (analogous to Figure 4 in the main text)
2. Figure S2: Same as Figure S1, but for CMIP5 models (analogous to Figure 5 in the main text)
3. Figure S3: Sahel region-mean zonal MSE advection profiles in the GFDL models, in the control simulations and in response to the imposed uniform SST warming (analogous to Figure 4 in the main text)
4. Figure S4: Same as Figure S1, but for CMIP5 models (analogous to Figure 5 in the main text)
5. Figure S5: Sahel region-mean convective mass flux profiles in those GFDL models for which it is available, in the control simulations and in response to the imposed uniform SST warming
6. Figure S6: Interannual covariances in observations and in the AMIP simulations of AM2.1, AM3, and HiRAM of Sahel region-mean precipitation with surface radiative fluxes (analogous to Figures 10-12 of the main text, combined)

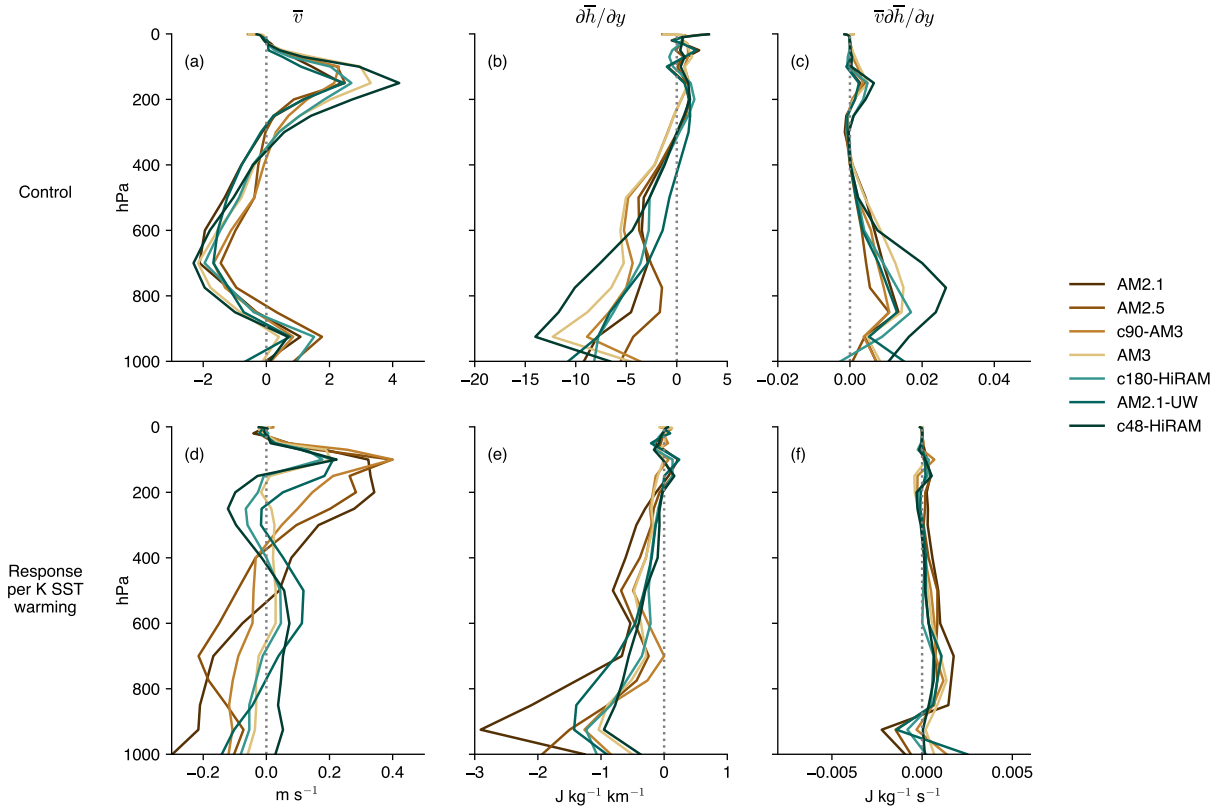

Figure S1: Meridional advection terms. This figure is identical to Figure 4 of the main text, except that in the right column horizontal (meridional plus zonal) advection is replaced by meridional advection.

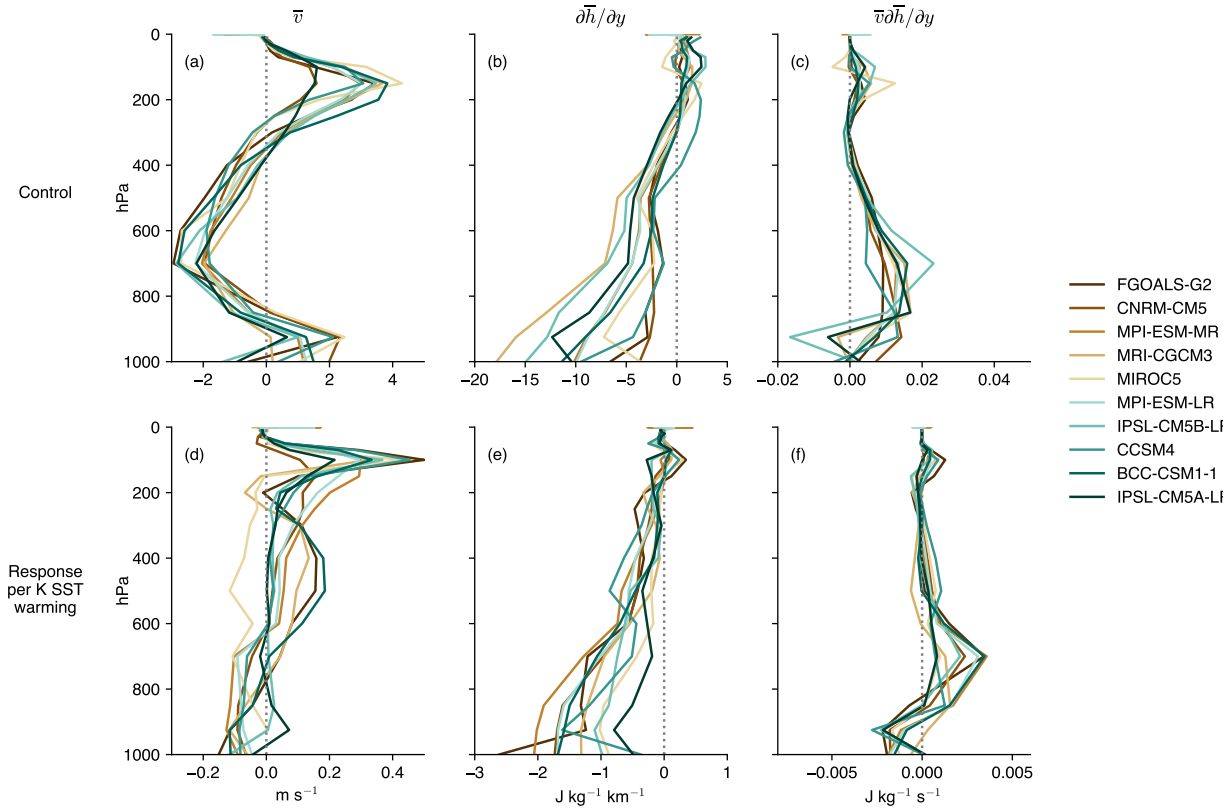

Figure S2: As in Figure S1, but for the CMIP5 models.

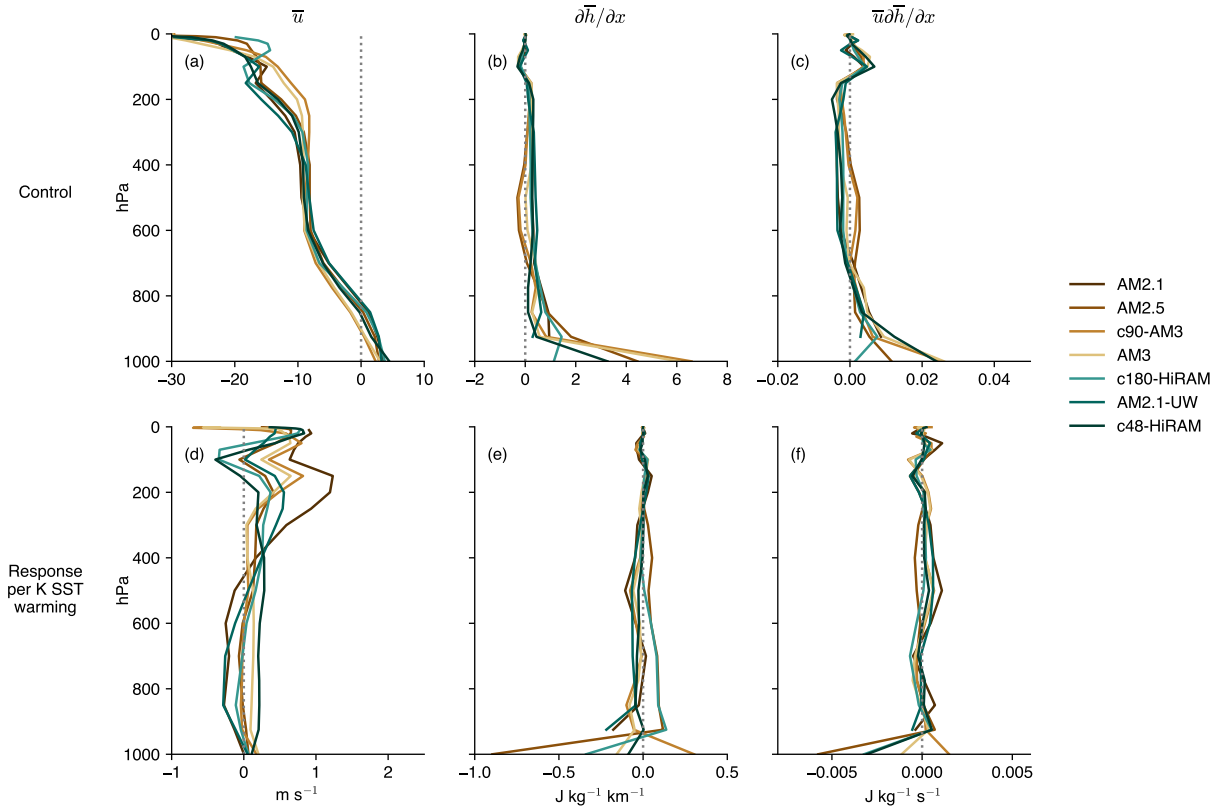

Figure S3: Zonal advection terms. For ease of comparison with the meridional advection profiles, the horizontal axis spacing in panels (c) and (f) are identical to the corresponding panels of Figures 4 and 5 of the main text.

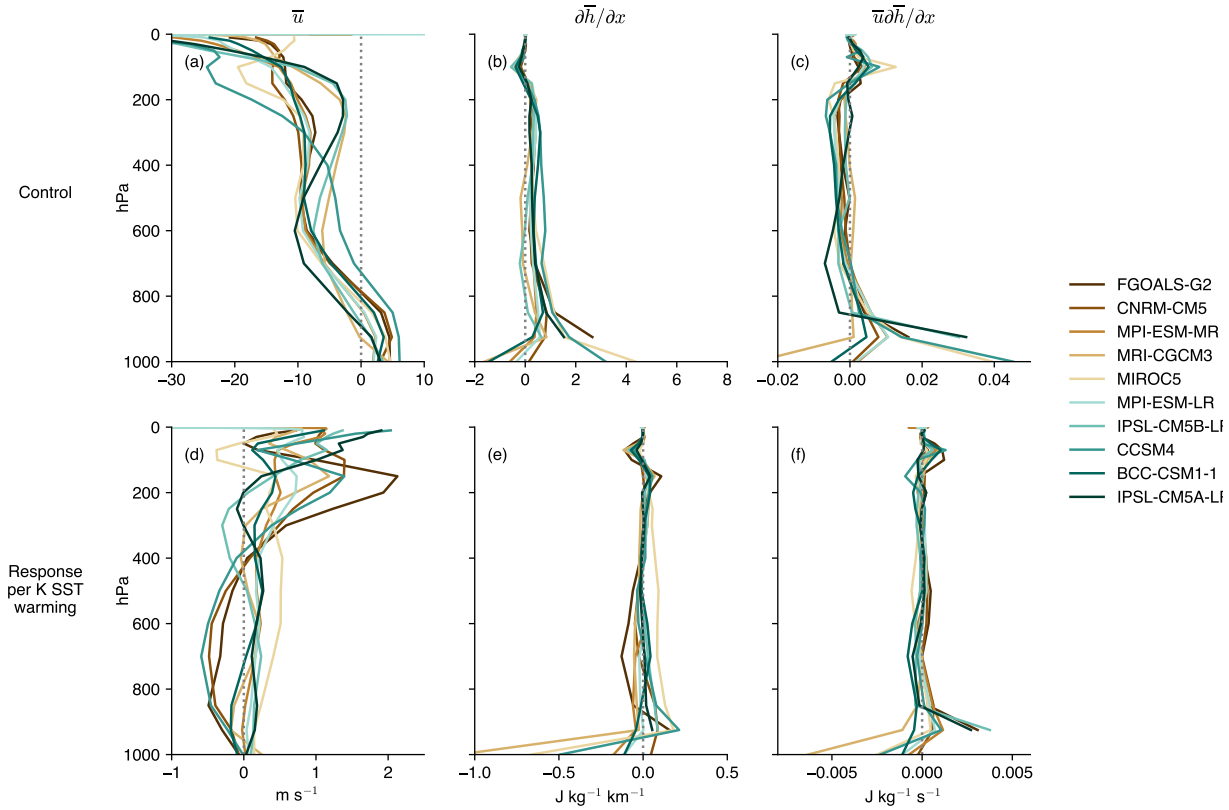

Figure S4: As in Figure S3, but for the CMIP5 models.

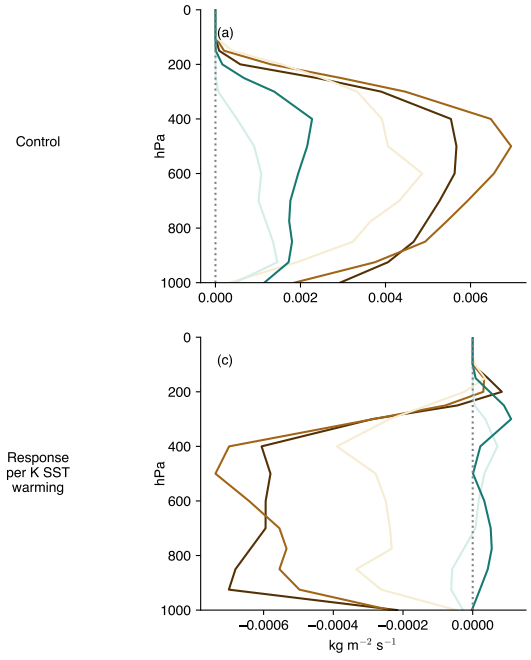

Figure S5: Sahel region-mean JAS convective mass flux profiles, in kg m^{-2} s^{-1}, in those GFDL models for which the data was available, in (a) the control simulation and (b) response per degree of imposed SST warming. Curves from brown to green: AM2.1, AM2.5, AM3, c180-HiRAM, and c48-HiRAM.

Figure S6 (on following page): Sahel region-mean (vertical axis) surface radiative flux and its components, in W m^{-2} and signed positive downward, as a function of (horizontal axis) precipitation, in mm day^{-1}. Columns from left to right: CERES-EBAF and CRU observational data; AM2.1 AMIP simulation; AM3 AMIP simulation, and c180-HiRAM AMIP simulation. Rows from top to bottom: all-sky net surface radiative flux, clear-sky net surface radiative flux, cloudy-sky surface radiative flux, cloudy-sky surface LW radiative flux, cloudy-sky surface SW radiative flux. Each dot represents a single year, and the overlaid gray line is the linear best fit. Also printed in each panel is the square of the Pearson correlation coefficient (r^2), the corresponding p-value based on a two-sided Student's t-test assuming each year is independent, and the slope of the best fit line, in W m^{-2} per mm day^{-1}. Red squares in (b)-(c) denote the equilibrium response in the uniform 2 K SST warming simulation in mm day^{-1} (not normalized by the SST warming). Compare to Figures 10-12 of the main text.

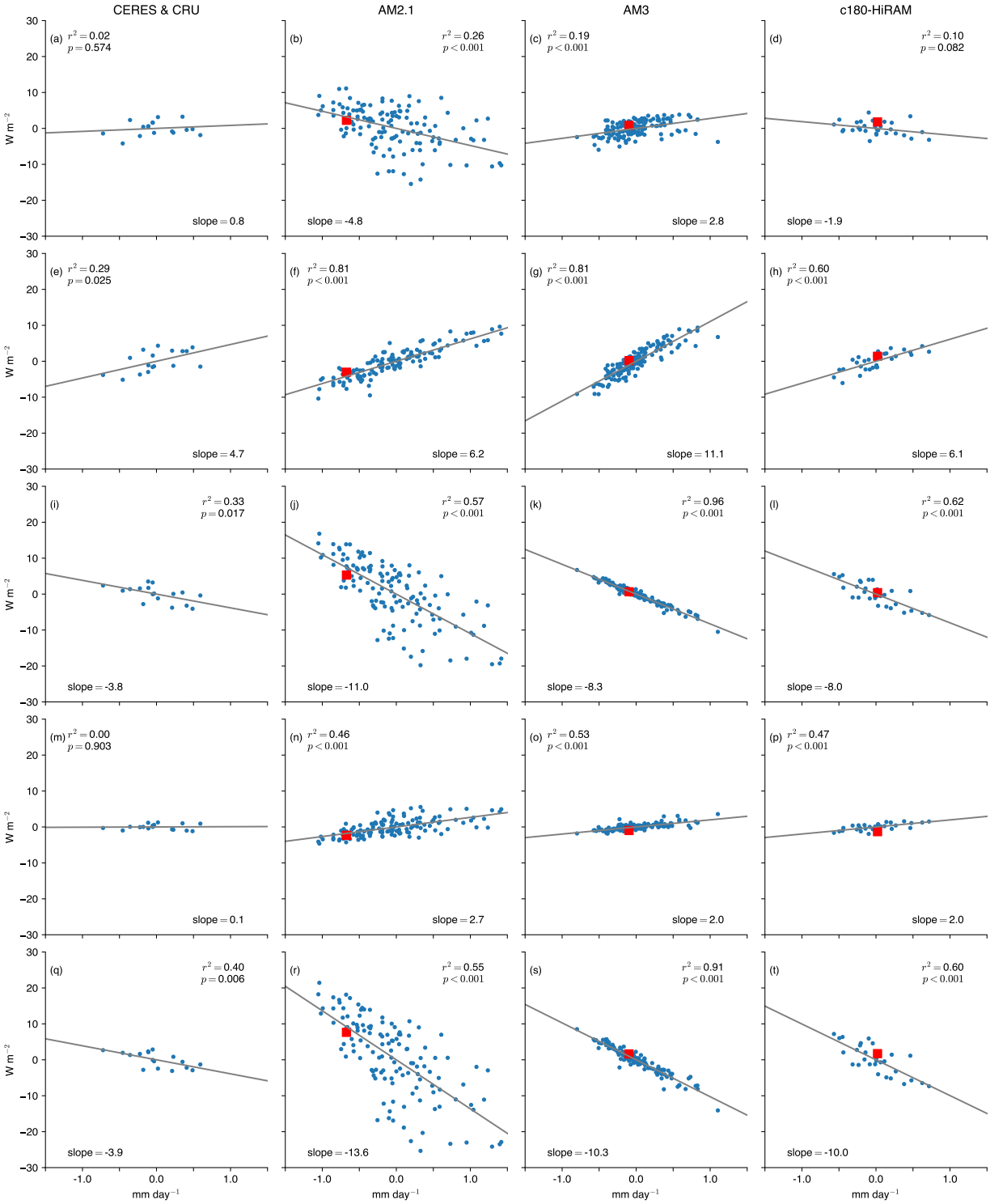
CERES & CRU
AM2.1
AM3
c180-HiRAM
(a) $r^2 = 0.02$ $p = 0.574$ slope = 0.8
(b) $r^2 = 0.26$ $p < 0.001$ slope = -4.8
(c) $r^2 = 0.19$ $p < 0.001$ slope = 2.8
(d) $r^2 = 0.10$ $p = 0.082$ slope = -1.9
(e) $r^2 = 0.29$ $p = 0.025$ slope = 4.7
(f) $r^2 = 0.81$ $p < 0.001$ slope = 6.2
(g) $r^2 = 0.81$ $p < 0.001$ slope = 11.1
(h) $r^2 = 0.60$ $p < 0.001$ slope = 6.1
(i) $r^2 = 0.33$ $p = 0.017$ slope = -3.8
(j) $r^2 = 0.57$ $p < 0.001$ slope = -11.0
(k) $r^2 = 0.96$ $p < 0.001$ slope = -8.3
(l) $r^2 = 0.62$ $p < 0.001$ slope = -8.0
(m) $r^2 = 0.00$ $p = 0.903$ slope = 0.1
(n) $r^2 = 0.46$ $p < 0.001$ slope = 2.7
(o) $r^2 = 0.53$ $p < 0.001$ slope = 2.0
(p) $r^2 = 0.47$ $p < 0.001$ slope = 2.0
(q) $r^2 = 0.40$ $p = 0.006$ slope = -3.9
(r) $r^2 = 0.55$ $p < 0.001$ slope = -13.6
(s) $r^2 = 0.91$ $p < 0.001$ slope = -10.3
(t) $r^2 = 0.60$ $p < 0.001$ slope = -10.0
W m^{-2}
mm day^{-1}